Int J Earth Sci (Geol Rundsch) (2017) 106:1453–1468
DOI 10.1007/s00531-016-1366-4

REVIEW ARTICLE

Review on symmetric structures in ductile shear zones

Soumyajit Mukherjee[1]

Received: 11 December 2015 / Accepted: 26 July 2016 / Published online: 13 July 2016
© Springer-Verlag Berlin Heidelberg 2016

Abstract Symmetric structures in ductile shear zones range widely in shapes and geneses. Matrix rheology, its flow pattern, its competency contrast with the clast, degree of slip of the clast, shear intensity and its variation across shear zone and deformation temperature, and degree of confinement of clast in shear zones affects (independently) the degree of symmetry of objects. Kinematic vorticity number is one of the parameters that govern tail geometry across clasts. For example, symmetric and nearly straight tails develop if the clast–matrix system underwent dominantly a pure shear/compression. Prolonged deformation and concomitant recrystallization can significantly change the degree of symmetry of clasts. Angular relation between two shear zones or between a shear zone and anisotropy determines fundamentally the degree of symmetry of lozenges. Symmetry of boudinaged clasts too depends on competency contrast between the matrix and clast in some cases, and on the degrees of slip of inter-boudin surfaces and pure shear. Parasitic folds and post-tectonic veins are usually symmetric.

Keywords Ductile shear zone · Symmetric clasts · Symmetry · Simple shear · Pure shear · Augen

Introduction

Kinematics of ductile shear zone is important to study seismicity and tectonics (Regenauer-lieb and Yuen 2003). Symmetric- and asymmetric structures can occur side by side in ductile shear zones (Nicolas 1987). Out of them, while several reviews on asymmetric structures/objects indicating ductile shear sense were made from time to time (Simpson and Schmid 1983; Hanmer and Passchier 1991; Goscombe and Passchier 2003; Passchier and Coelho 2006 etc.), symmetric structures/objects, inside ductile shear zones with prominent shear sense indicators (Mukherjee 2014, 2015), have received less attention: For example, it has been missed in the recent book on ductile deformation by Hobbs and Ord (2014). However, a wealth of rheological and kinematic information has been deduced from such objects in natural ductile shear zones (this review). Symmetric structures have been described in structural geology in terms of augen, clasts, lozenges, boudins and folds. This work reviews such symmetric structures, and cites examples from Himalayan shear zones. Ductile shear zones developed by glacial flows (e.g. van der Wateren et al. 2000) and landslides (e.g. Philips 2006) are not discussed here.

Symmetric structures in ductile shear zones

Augen

Lens-shaped/elliptical/lenticular clasts (Fig. 1), commonly of K-feldspars, either single minerals or aggregates, have classically been described as "augen" (singular form: "auge": Winter 2009; synonym "phacoidal": Spry 1974) that may have an "outer metamorphic rim" (Passchier et al. 1990) and found in quartz biotite muscovite bearing gneisses, mafic gneisses and meta-granitoids up to moderate shear strain and except those formed at low temperature (Barker 1998), granulites (White 2010 and references

✉ Soumyajit Mukherjee
soumyajitm@gmail.com

[1] Department of Earth Sciences, Indian Institute of Technology Bombay, Powai, Mumbai, Maharashtra 400 076, India

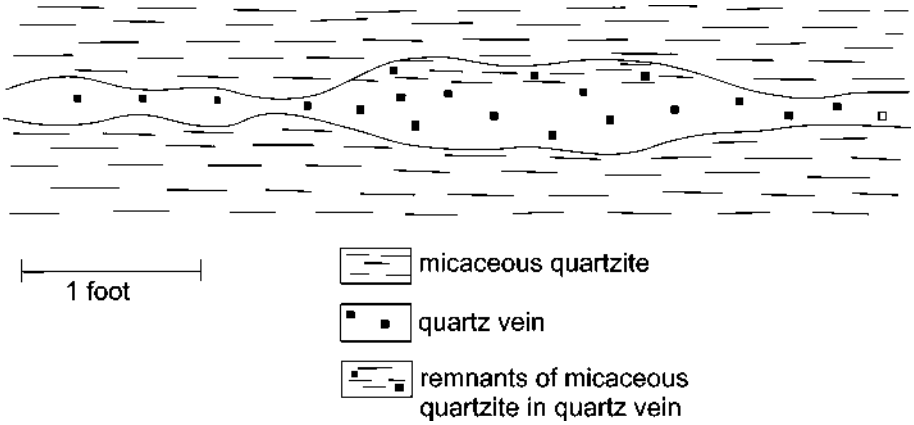

Fig. 1 Pure shear on a layer of rock produces symmetric pinch and swell structures. Reproduced from Fig. 111 of Ramberg (1952)

therein), amphibolites mylonites (Leiss et al. 2002), schists (Vernon 2004), augen mylonites/blastomylonites (Bucher and Grapes 2011), dynamically metamorphosed granites (Roshoff 1979), possibly sheared schists softened by pegmatitic fluids (Barbour 1930 and references therein) that plausibly supplied K-feldspar during shear (Cannon 1964) etc. Augen of perthites might alter to other variety of feldspar by deformation (Smith 1974 and references therein). Feldspar augen are usually inside matrix of other minerals such as quartz. Vidal et al. (1980), however, reported feldspar augen within feldspar rich matrix from southern France. Chlorites, micas and hydrogarnets can also develop augen (Augustithis 1979). The word augen has also been used to describe rectangular and euhedral clasts (Vernon 1986).

Augen gneiss can be produced by deformation of both porphyritic and porphyroblastic rocks of igneous and metamorphic origin, respectively (Vernon and Clarke 2008). Augen have been debated to have either syntectonic or post-tectonic growth (Passchier et al. 1990). Ramberg (1952) considered some augen to be porphyroblastic, although syn-to-post-crystalline deformation can fragment them. Boudinaging and intense (dynamic) recrystallization concomitant to ductile shear on initially larger feldspar clasts can modify original margins of grains into lens-shaped porphyroclasts. Modification of grain margins might happen with pegmatite veins as well. Myrmekitization is another way to reduce grain size of feldspar (Ree et al. 2005 and references therein) coeval to ductile shear and at higher pressure sites of feldspar grains (Simpson and Winsch 1989). Augen of feldspar can be produced by myrmekitization either by replacement or by exsolution with a dominant role of fluids involving volume loss in ductile shear zones (Menegon et al. 2006, 2008; Ishii et al. 2007). Compositional patches/flasers in rocks of lenticular geometry such as augen indicate their origin from larger grains (Fry 1997). Feldspar augen can have recrystallized margins (Hollocher 2014) indicating grain size reduction. The recrystallized minerals surrounding augen may contain neograins/subgrains (Vidal et al. 1980). The central part/core of augen might indicate equilibrium recrystallization (Vidal et al. 1980). If the synkinematic theory of genesis of augen is to be agreed, deformation distributed inside the rock and recrystallization occurred along specific directions (De Sitter 1956).

Alternately, augen could be phenocrysts of residual magmas (Vernon 2004; see Chattopadhyay et al. 2015). Vernon (1990) after reviewing feldspar augen considered those to be residual phenocrysts and not porphyroblasts. In a way, he negated boudinaging of veinlets during deformation as the other possible genesis (Kornprobst 2002). Magmatic flow layers may consist of oriented prismatic crystals (Turner and Verhoogen 1951) and might be considered as augen that would not always give any shear sense.

As recrystallization rates of clasts fall with increasing shear/mylonitization (Hooper and Hatcher 1988), the chances of producing mantled clasts also keep reducing. Although a few augen might be deformed (Roshoff 1979), those are mostly resistant minerals of initially undeformed rocks that withstood mylonitization (Davis et al. 2012). In turn, augen also create synshear heterogeneous flow field (Bouchez et al. 1987). Together with kink folds, augen have been considered to indicate inhomogeneous deformation (Dell'Angello and Tullis 1989). Pure shear can partially melt layered sedimentary rocks and produce near-symmetric elliptical pods of solidified materials, similar to augen (Mason 1978). Masuda and Mizuno (1995) modeled symmetrically distributed softer materials around rigid clasts, similar to phi-structures as referred in Passchier and Trouw (2005). A few earlier workers such as Hills (1963) mentioned elliptical symmetric quartz blebs to be products of flattening/pure shear of host rocks. Interestingly, even earlier than Hills (1963), Ramberg (1952) in his Fig. 72 supported pure shear origin of some augen (Fig. 1). Augen mylonites on pronounced flattening, however, form banded mylonites (Simpson and Winsch 1989) destroying the

augen geometry. Sometimes augen have inclusions in specific zones that are easy to identify under an optical microscope (Vernon 1986 and references therein), but the inclusion patterns may not indicate shear sense (e.g. Fig. 1.50 in Mukherjee 2013a).

Lenticular mineral fish defined either by a single or an aggregate of minerals morphologically come under the augen category (Lister and Snoke 1984; Mukherjee 2011a). The long axes of such grains, if inclined to the primary shear C plane, indicate ductile simple shear sense (examples in Vernon 2004 and Mukherjee 2013a). In some cases, the axis however parallels the C plane. In those cases, no shear sense is indicated. ten Grotenhuis et al. (2003) included such fish into Group 1 and 5 categories. Such mineral fish are devoid of pressure shadows at two sides. Individual mineral grains in composite mineral fish do not indicate the true ductile shear sense (Mukherjee 2011a).

Clasts without and with mantles

Passchier and Trouw (2005) used the term "naked clasts" to describe porphyroclasts with prominent margins and no tails/wings. Tails are *"…appendages present on both sides of porphyroclasts trending parallel to the foliation"* (Passchier and Trouw 2005). Thus, the term "naked clast" is an implicit renaming of few augen structures. Hornblende being stronger than feldspar, the former forms naked clasts more efficiently within fine-grained matrix (Trouw et al. 2010). Bons et al.'s (2008) analog modeling inferred that augen/clasts without tails develop when eye-type flow pattern appear by simple shear with separatrices forming much away from the augen/clasts. Earlier to this work, however, Marques et al. (2005) pointed out that the flow pattern depends additionally on the ratio between the width of the shear zone and the least axis of the clast.

Nicolas (1987) considered implicitly phi-type clasts as augen. Phi-type clasts, one of the four types of mantled porphyroclasts, in high-grade coarse grained mylonites devoid of stair step with symmetrically deflected main foliations (Fig. 2) have been described as "winged mantled clasts" (Passchier and Trouw 2005). On deformation, wings might alter morphologically but the clasts simply reduce size (Passchier and Trouw 2005). Numerical models of pronounced ductile shear on mantled clasts with high mantle width can produce symmetric phi-structures. Quarter folds may develop around symmetric clasts. In this case, the ductile shear sense is deduced solely from the fold asymmetry (as in Passchier and Trouw 2005), and *not* from the clast. The situation is similar to Simpson and Schmid (1983) Fig. 4d that shows a rotated garnet porphyroblast but with near-symmetric pressure shadow. The pressure shadow being symmetric does not give shear sense. Rather only the inclusion pattern inside the garnet does.

Cliff and Meffan-Main (2003) referred formation of core and mantle structures with quartz-feldspar mosaic in the mantle from Alpine shear zones as the trigger for augen/naked clast formation. Winged clasts form from a low competency contrast between the mantle and the matrix

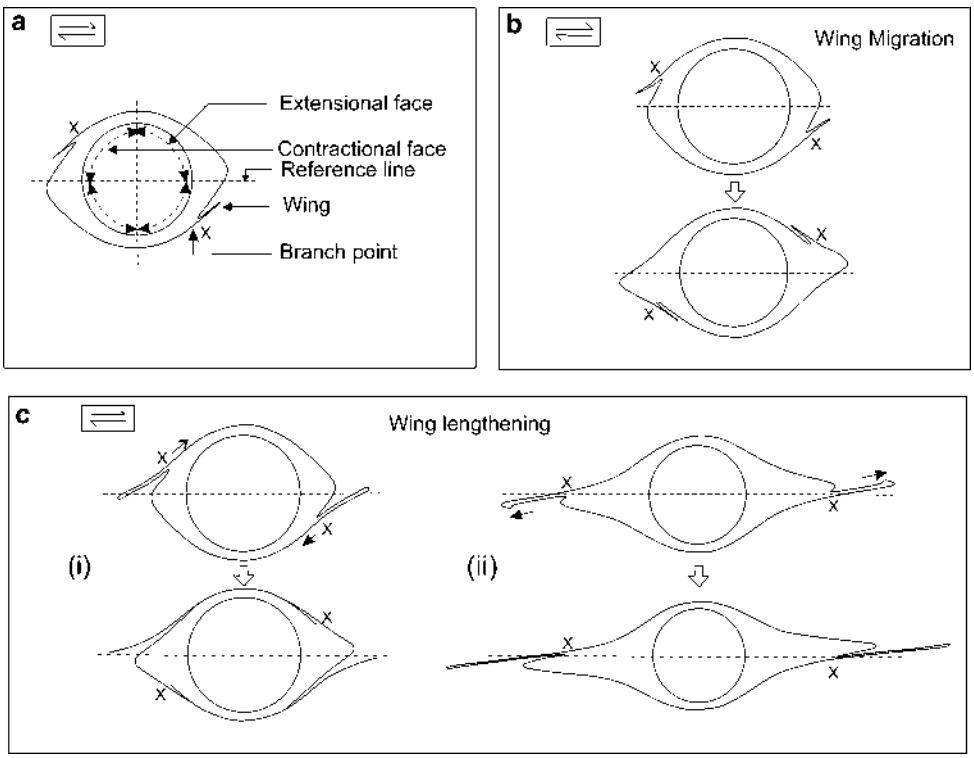

Fig. 2 *Mantle structure:* mantle around core. *Tails:* deformed mantle at both sides of the core. *Wing: narrow* extensions of a tail (Fig. 2a). *Branch Point:* the point from which a wing tail's offshoot. *Wing migration:* wing's movement together with the branch point (Fig. 2b). *Wing lengthening:* increment in wing's length by two methods: branch point transfer (1) but no wing lengthening, and (2) with lengthening (Fig. 2c). Contractional face and extensional face: parts of the object that temporarily face the contractional and extensional fields, respectively. Reproduced from Fig. 2 of Mandal et al. (2000)

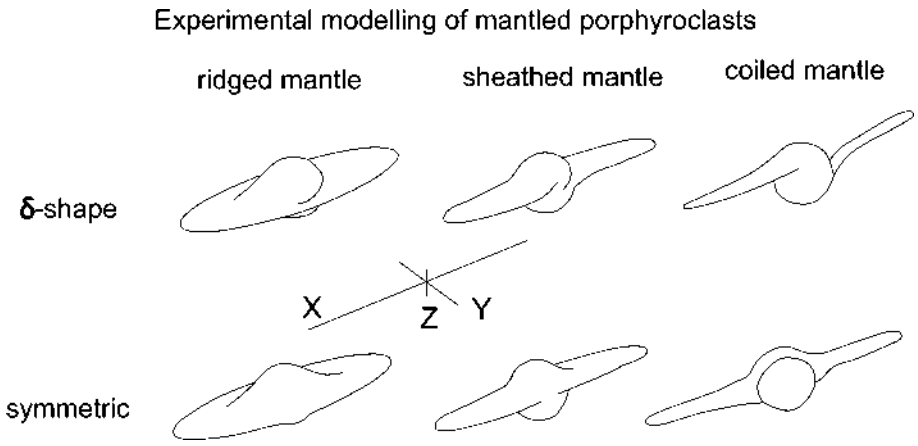

Fig. 3 Types of clasts with winged mantles in analogue models. Reproduced from Fig. 9 of Passchier and Sokoutis (1993)

(Passchier and Sokoutis 1993). Had there been a much disparity of competency, winged clasts do not form. Difference in stress produced inside the matrix, if non-Newtonian can govern the mantle geometry (Passchier and Sokoutis 1993), and in general, grain size in the matrix (Trouw et al. 2010). On contrary, however, Bons et al. (1997) mentioned that the flow field, and hence the clast–mantle geometry, more fundamentally depends on the boundary condition and not on the rheology. For example, an eye-shaped flow pattern is developed around a clast with boundaries of the shear zone far away, whereas if the boundary is close to the clast, a bow-tie shaped flow field would develop (Bons et al. 1997). Passchier and Sokoutis (1993) classified symmetric mantles into three types: ridged mantle, sheathed mantle and coiled mantle (Fig. 3). In all cases, tails extend across the clast at two opposite sides. The extent of tails for ridged mantle perpendicular to elongated side (the Y-direction in Fig. 3) is maximum, for sheathed mantle it is moderate, and for coiled mantle it is least. The coiled variety of mantle develops in a more viscous medium (Passchier and Sokoutis 1993). Bellot et al. (2002) considered symmetric pressure shadows and pressure fringes not giving shear sense (such as Figs. 4, 5) as products of pure shear. Boundaries of symmetric minerals, surrounding which pressure fringe is defined, can either be parallel to the external foliation (B1 in Fig. 4), or at an angle (B2 in Fig. 4). Likewise, the fiber minerals for symmetric mineral fringe either parallel the external foliation (B1 in Fig. 4), or at an angle (B2 in Fig. 4). Ishii (1995) simulated symmetric pressure fringe around rigid circular clasts for pure shear deformation. For elliptical clasts with long axes either parallel or perpendicular to the main foliation (/primary shear plane/C plane), pure shear also produces fringe at the two opposite sides of the clast symmetrically. If the long axis, however, initially is inclined at other angles with the C plane, asymmetric structures form by pure shear (Fig. 4 in Ishii 1995).

Both simple and compound pressure fringes can be symmetric, and produced by pure shear leading to inhomogeneous strain (Spry 1974). The following statements can further be made from Spry (1974): The fiber axis of a pressure fringe is the orientation of the flaky minerals that can either be straight or curved. Straight fibers usually indicate pure shear. As rotation of grains, surrounding which fringes are defined, is possible under pure shear as well, such rotated grains do not necessarily indicate pure shear. The segment junction, defined as a line separating fibers of two different orientations, may (1–3 in Fig. 4c) or may not (4 and 5 in Fig. 4c) parallel the external foliation (Se). A pure shear in particular can produce pressure fringe with parallel fibers (Fig. 8.2 caption in Nicolas 1987). Can we at all discriminate symmetric pressure fringe produced by pure shear in that case? Kanagawa (1996) pointed out that symmetric straight syntaxial and antitaxial fibers would indicate pure shear. Notice that Koehn et al. (2001) numerically simulated symmetric pressure fringe similar to case (3) of Fig. 4c.

Whereas wings initially parallel the direction of maximum instantaneous extension, depending on the recrystallization rate and the strain rate, several geometries of wings can evolve (Passchier 1994). The ratio of mantle-to-the core material is governed primarily by the recrystallization rate (Passchier 1994). A significantly bigger core can protect the mantle from getting sheared (Passchier 1994). A leisurely recrystallizing clast attains a theta geometry (Passchier 1994). On the other hand, analytical modeling of general shear of inequant clasts within a Newtonian matrix led Mandal et al. (2000) to conclude that the mantle geometry, whether symmetric or asymmetric, is primarily controlled by (1) the aspect ratio of the clast before deformation started; (2) rate of fall of clast size; and (3) kinematic vorticity number (i.e. ratio of simple-to-pure shear).

Curvature of tails can indicate deformation type. For example, straight tails indicate that the bulk rock underwent a pure shear, and curved tails a simple shear (Spry 1974). Passchier (1994) explained different types of porphyroclasts in a single rock sample in terms of the shape

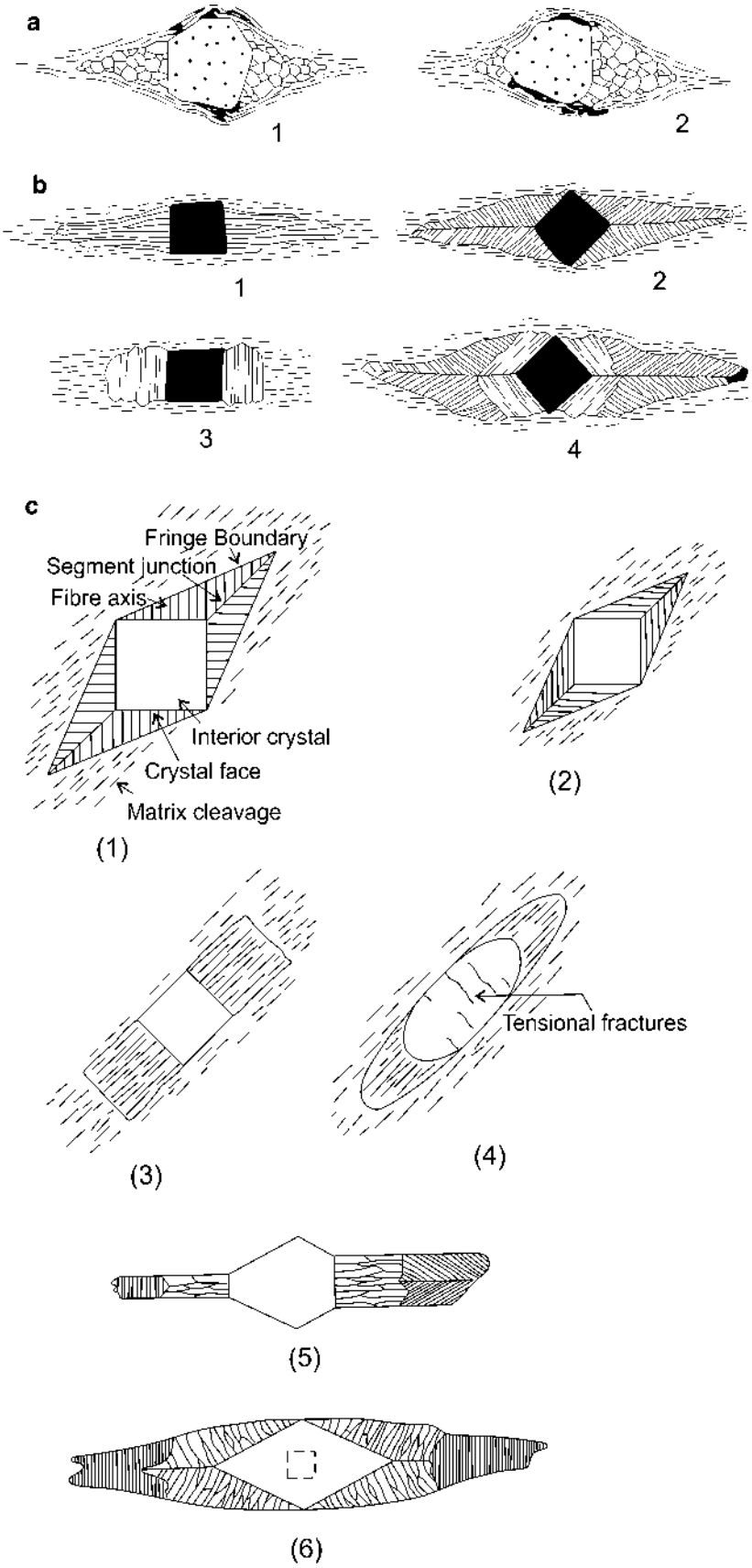

Fig. 4 **a** Near-symmetric pressure shadows at the two sides of clasts in ductile shear zones: **b** Pressure fringes: (1) simple type, (2) composite type, (3) simple with micaceous lamellae, (4) composite with mica and quartz. Reproduced from Fig. 5.10 of Bard (1986). **c** Different morphological varieties of pressure fringes, reproduced from Fig. 56 of Spry (1974)

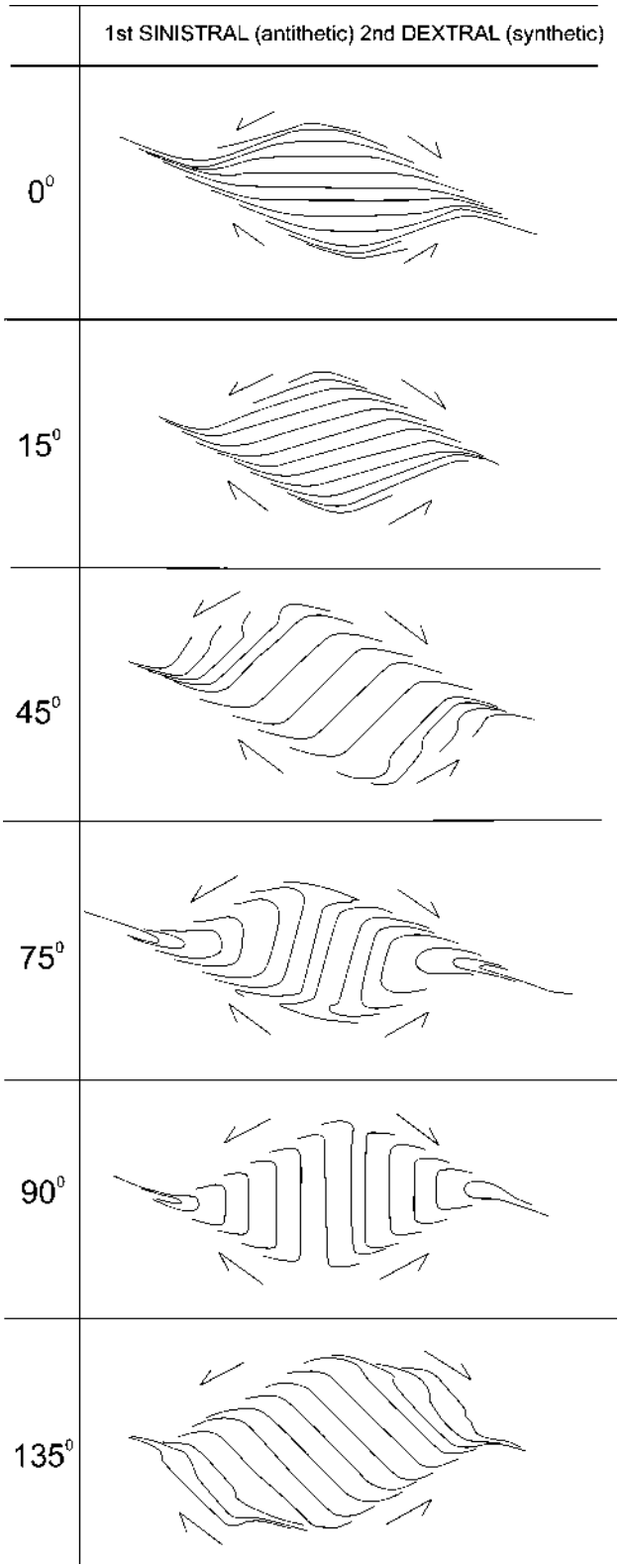

Fig. 5 Internal morphology of lozenges produced by intersecting shear zones inside anisotropic and homogeneous medium. Angles between the primary shear plane, here the *horizontal* direction and the internal fabrics are stated. Reproduced from Fig. 3.33 of Ponce (2014)

of the separatrix and how much it intersects the mantle. For example, if a wide mantle engulfs the separatrix completely, wings develop eventually.

Bjornerud (1989) in his Fig. 3 designated near-symmetric objects in ductile shear zones as "category-i" objects. These are produced when both the object-matrix boundary gradient (decided by the slip potential of the object with respect to the matrix) and the shear-rate gradient across the ductile shear zone are (qualitatively) moderate. In such a case, the object undergoes partial rotation within the matrix and attains a symmetric position that does not give a clear shear sense.

Temperature of deformation and intensity of shear can guide whether symmetric or asymmetric structures would develop/evolve. For example, (1) Ductile shear sense indicators reduce in number as rocks undergo low grade (250–500 °C) to medium grade (500–650 °C) and then to high-grade (>650 °C) metamorphism. Thus, as temperature rises, more symmetric objects usually develop in ductile shear zones: As Trouw et al. (2010) concluded qualitatively based on microstructural observations. A temperature rise at nearly the same confining pressure would be possible if magmatic melt intrudes a deforming shear zone, such as what happened during mid Miocene period at the South Tibetan Detachment System at the northern margin of the Greater Himalayan Crystallines (review in Yin 2006; Mukherjee 2013b). A second source of heat could be the shearing event itself, i.e. the viscous dissipation/shear heat (Nabelek et al. 2010; Mukherjee and Mulchrone 2013; Mulchrone and Mukherjee 2015). Asymmetric objects have been indeed reported from this detachment zone by fieldwork and thin-section studies from Sutlej (Mukherjee and Koyi 2010a), Zanskar (Mukherjee and Koyi 2010b) and Bhagirathi river sections (Mukherjee 2013c, d, 2014) of western Indian Himalaya. Therefore, it appears that higher temperature promotes greater synshear mobility of materials. (2) Prolonged ductile shear can transform an asymmetric shear sense indicator into a symmetric structure and then again into another asymmetric structure. For example, in general, a delta structure on higher strain evolves into a phi-structure, when eye-shaped flow perturbation develops (Passchier 1994). On still higher strain, the phi-structures can become a sigma structure (Mandal et al. 2000). Geometric changes from one clast geometry into another, and thereby change in degree of symmetry, is also possible if the recrystallizing clast keeps supplying mantle material during deformation (Passchier 1994). Note that Bose and Marques (2004) pointed out an additional constrain of degree of slip between the clast and the matrix in generating the flow pattern.

Lozenges

Ponce et al. (2013) used the word "tectonic lozenges" to include scale- and genesis-independent rhombic, lensoidal,

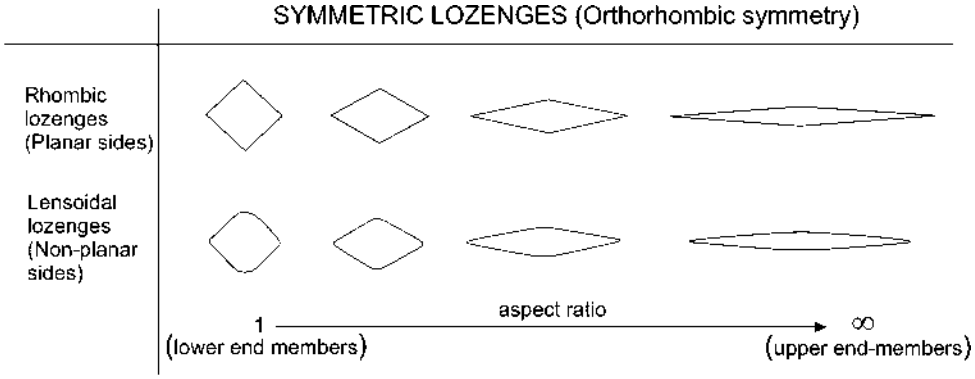

Fig. 6 Lozenges as per symmetry. Nearly linear margins. Reproduced from Fig. 1 of Ponce et al. (2013)

rhomboidal and sigmoidal structures of minerals/rock units that are more competent than that matrix (Fig. 6) (also see Mukherjee 2013a, b, c, d). Notice that the term lozenge has also been used to describe brittle shear zone related rock slices (Awdal et al. 2014) that we do not discuss here. Lensoidal lozenges in one way are augen. Lozenges in ductile shear zones best develop in well-foliated and anisotropic rocks both by pure and simple shear (Ponce 2014). Lozenges produced by different mechanisms can have similar geometries. Lozenge-shaped rock units can also be produced by interaction between earlier phase secondary ductile ($C'$and C'') and later secondary brittle shear planes (R, R'). Analog modeling by Ponce (2014) indicate that an inclusion stiffer than the matrix would rotate instead of internally strained and produce lozenge. The central portion of the lozenges strains less than the marginal parts (Ponce 2014), same as that for some augen. In Ponce's (2014) models (Fig. 7), depending on (1) shear zone orientation with respect to planes of anisotropy in rocks, and (2) angular relation between cross-cutting shear zones, near-symmetric lozenges develop in 3D, can alter from one geometry into another. It is well known that simple shear on various clast sizes can produce asymmetric structures (Treagus and Lan 2003). Note that significant pure shear alone can also bring asymmetry of initially squarish clasts if embedded in a matrix of considerable different viscosity (Treagus and Lan 2000). Therefore, statements such as "symmetric clasts exclusively indicate pure shear" are incorrect.

Boudins

Clasts of non-Newtonian rheology embedded in another non-Newtonian material upon extension first develop boudins of symmetric necking. However, as extension intensifies, asymmetry may develop in boudins (Duretz and Schmalholz 2015). Stress applied parallel to foliation planes (i.e. buckle folding) can produce either symmetric folds or pinches and swells (Cosgrove 2007; Fig. 8). These folds are not produced by any ductile shear, and conversely their minor asymmetry does not reveal any shear sense. Pure shear can produce highly convex bulging symmetric boudins (Maeder et al. 2009). Weavy plagioclase layer within quartz rich rock under pressure perpendicular to the length of the layer (i.e. pure shear) can promote chemical alteration near the margin of feldspar grains and result in pinch and swell structure, i.e. augen connected by tails (as per Fig. 8 of Simpson and Winsch 1989). Pinched and swelled rock/mineral bodies, also referred as "winged inclusions", were shown in 2D finite element models of both Newtonian and non-Newtonian rheology, that on non-coaxial shear, such inclusions can alter from symmetric to asymmetric variety (Fig. 9; Grasemann and Dabrowski 2015).

Near-symmetric bone-shaped boudins might be produced by rotation of veins that were initially at an angle with their present orientation (Maeder et al. 2009): an incident presumably independent to matrix rheology (Kenis et al. 2006). Asymmetric bone-shaped boudins at an angle to foliation planes, on the other hand, give ductile shear sense (Malavielle and Lacassin 1988).

Boudins not produced by layer parallel extension, but by simple shear are called false boudins (Bons et al. 2004) or pseudo boudins (Passchier 2008). Besides ductile shear, false boudins are manifestations of magmatic intrusion, local expansion and collapse of magmatic bodies (personal communication with David Iacopini). Some of these boudins are symmetric and lenticular with long axes parallel to the main foliation. Symmetric foliation boudins (Fig. 10), one of the five types of foliation boudins, consist of lozenge-shaped veins in necks with symmetric cusps across them (Arslan et al. 2008). Fractures may cut such boudins at high angle to the foliation planes (Lacassin 1988).

Goscombe et al. (2004) referred that orthorhombic symmetric boudins might occur alongside asymmetric boudins, and that the former is produced from the kinematics of "no slip boudinage" where the inter-boudin surfaces did not undergo any slip. Natural boudins produced by either synthetic or antithetic slip are asymmetric (Dabrowski and Grasemann 2014). If considered alone, scar folds can be symmetric (Goscombe et al. 2004) such as those associated with some rectangular, barrel-shaped, lenticular,

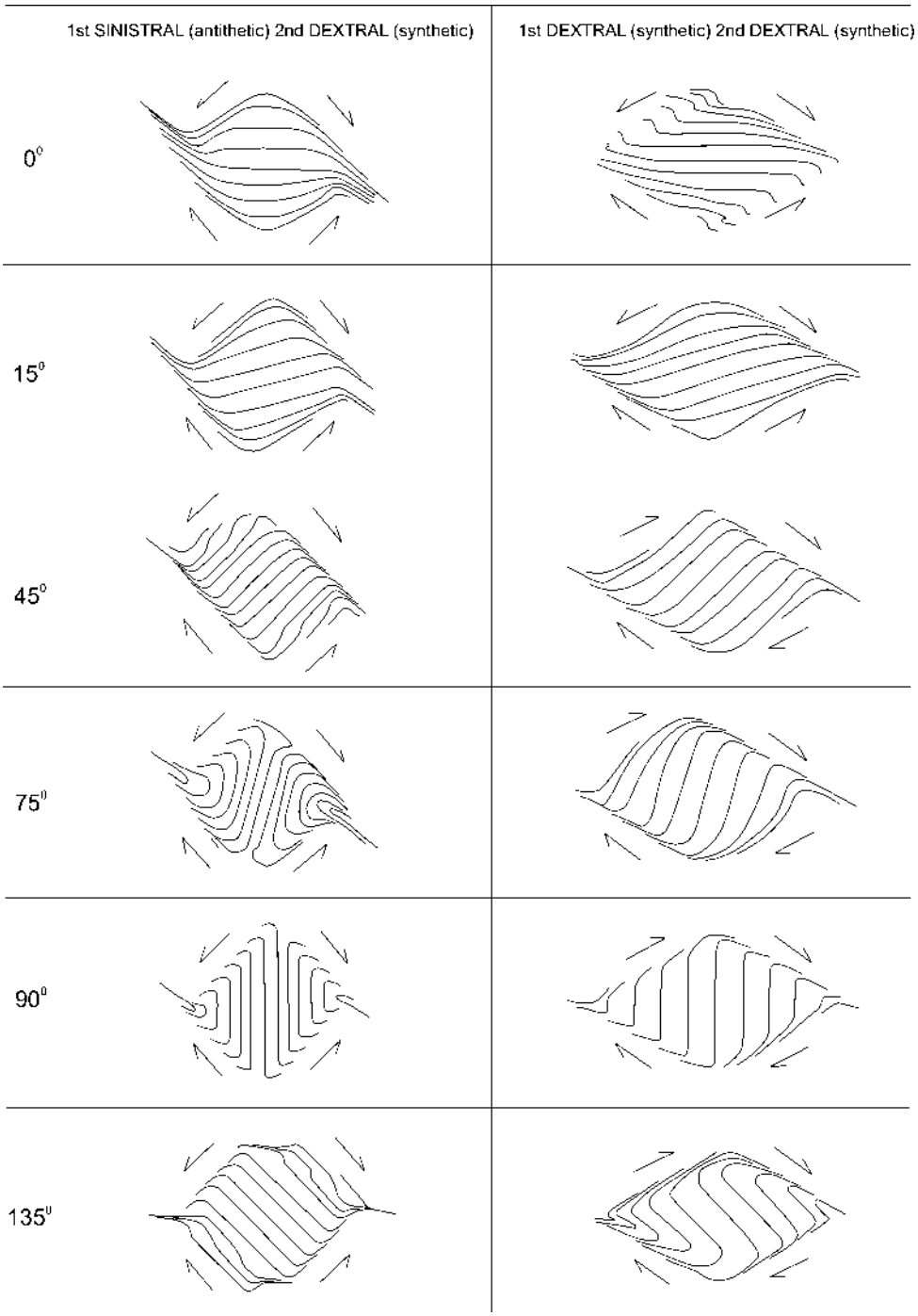

Fig. 7 Internal morphology of lozenges produced by intersecting shear zones inside anisotropic and homogeneous medium. Angles between the primary shear plane, here the *horizontal* direction, and the internal fabrics are stated. Reproduced from Fig. 3.32 of Ponce (2014)

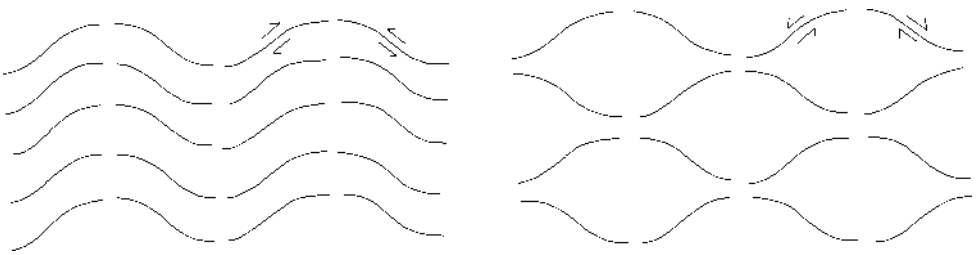

Fig. 8 Compression leading to folding and pinch and swell structure. Reproduced from Fig. 4a, b of Cosgrove (2007)

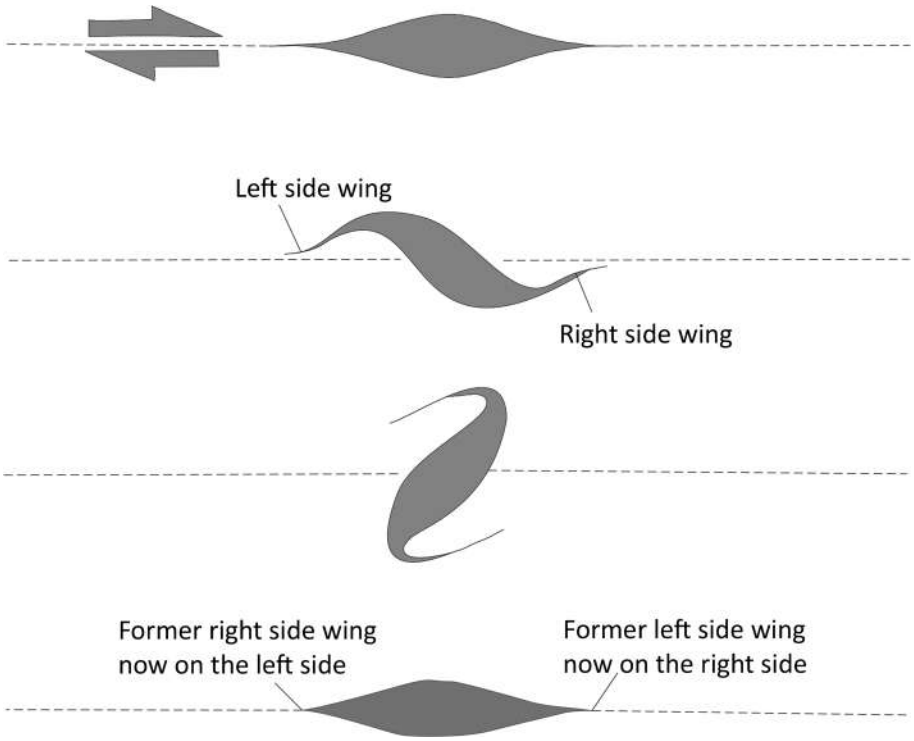

Fig. 9 Analytical models of ductile shearing on winged inclusions. Both the wings and the inclusions rotate. After pronounced rotation, wings swap their positions. Reproduced from Fig. 1c of Grasemann and Dabrowski (2015)

fish-head and rhombic boudins (Fig. 17.6 of Ghosh 1993) with notches/fish mouth (Whitten 1966). Numerical modeling revealed that the matrix rheology seems not to be the deciding factor of geometry of these boudins (Abe and Urai 2012; Fig. 11). Hollocher (2014) reported symmetric subcircular boudins of eclogite. Symmetric boudins with subcircular geometry are rare.

Folds and veins

Ductile shear induced folds are asymmetric and might be overturned and intrafolial in nature (Mukherjee 2015). On the other hand, parasitic folds of a lower order fold not affected by ductile shear are symmetric (Mandal et al. 2004). Newtonian viscous layer under pure shear within a non-Newtonian matrix may form symmetric folds (Ord and Hobbs 2013). Veins that parallel main foliations in sheared rocks could be symmetric, produced by hydraulic fracturing, and assisted by dissolution recrystallization of quartzofeldspathic minerals (Fig. 2 and references of Le Hebel et al. 2002). Veins cutting main foliations (primary shear C planes) can be asymmetric (Figs. 3.27, 3.28 and 3.30 in Mukherjee 2013a, b, c, d), or symmetric also.

Natural examples

Symmetric objects in ductile shear zones can be illustrated using natural examples (Figs. 12, 13, 14, 15). Many of these examples (Figs. 12, 13b, d, 14a, b, d, 15) come from Archean–Proterozoic greenschist-amphibolite facies (migmatitic) gneisses of the Greater Himalayan Crystalline rocks from the western Indian Himalaya from Sutlej, Zanskar and Bhagirathi river valleys (Yin 2006; Mukherjee 2013a, c; Mukherjee and Koyi 2010a, b for general geology). An single example (Fig. 14c) comes from Paleozoic-Mesozoic metamorphic belt of Pangong Tso Group of mylonite and another (Fig. 13c) from Tangste Group of high-grade metamorphic rocks near the Shyok Suture Zone (Ladakh, India). These two groups of rocks are exposed within the Karakoram Metamorphic Complex at the southern portion of the Eurasian plate (general geology reviewed in Jain and Singh 2008). Figure 13a provides an example from ductile sheared Proterozoic-Paleozoic orthogneisses from Tso Morari Crystallines (regional geology reviewed in Jain and Singh 2008; Mukherjee and Mulchrone 2012).

Figure 12a depicts a lenticular augen of quartz with subtle internal foliation planes developed that parallel the main foliation within the rock matrix. This is similar to the Si-Se concordance situation studied in porphyroblast-matrix relationship where syntectonic growth of the augen can be ascertained (as reviewed in Passchier and Trouw 2005). However, not always internal foliations can develop inside augen that could be rhombic with sharp margins with minor curvature, such as Fig. 12b, which resemble a lensoidal lozenge with moderate aspect ratio such as Fig. 6 (Ponce et al. 2013). Augen in Fig. 12a, b might also indicate pronounced ductile shear, similar to Grasemann and Dabrowski (2015),

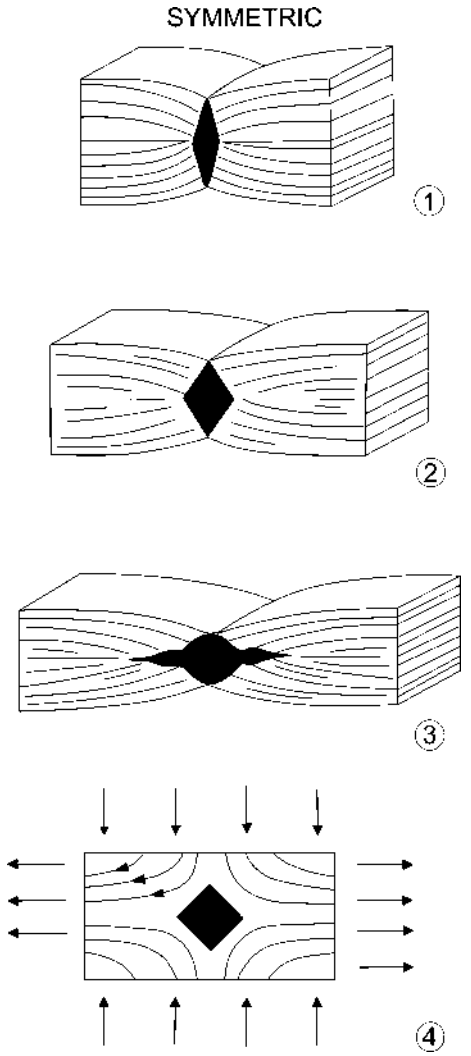

Fig. 10 Pure shear and progressive development of foliation boudins. Reproduced from Fig. 5a of Lacassin (1988)

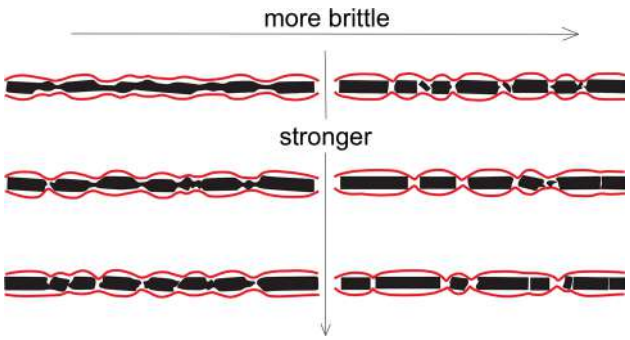

Fig. 11 Models with different rheology of the extended layer. Matrix material, however, is of the same Mohr–Coulomb rheology. Reproduced from Fig. 10 of Abe and Urai (2012)

whereby those augen at some part of deformation history were asymmetric (compare with Fig. 9). This symmetric and porphyroblastic augen not showing any shear sense might exist aside a ductile sheared sigmoid clast (Fig. 12c). This presumably indicates inhomogeneous nature of deformation, as predicted by Bouchez et al. (1987) that sometimes happen around augen. Augen may pinch a little near the central part and display tail at one of its side with the same mineral species as the augen itself (Fig. 12d).

In microscale, symmetric clasts with and without mantles can be appreciated better. Figure 13a shows a garnet porphyroblast with irregular margins. Retrogressed chlorite skirts this grain and is extended a bit along the main foliation defining a theta structure. Unlike Fig. 2 (Mandal et al. 2000), wings did not develop in the chlorite tails. Taken the garnet and the chlorite grains together, the structure is comparable with "symmetric coiled mantle" as in Fig. 3 (Passchier and Sokoutis 1993) indicating a viscous matrix. In this case, garnet upon retrograde metamorphism supplied chlorite to form the short tails. This is comparable with Ree et al.'s (2005) cited example where myrmekitization of feldspar grain supplied material for the mantle material of the feldspar augen. Notice that porphyroblast may not always contribute to form tails by chemical alteration at its margin: For example, Fig. 13b shows a square-shaped garnet grain with pressure symmetric shadows at two sides. Unlike cases A1 and A2 in Fig. 4 (Bard 1986), here sizes of quartz grains in the two pressure shadows are quite different. Even then, such symmetric shadow might indicate a component of pure shear, as postulated by Bellot et al. (2002). The nearly straight tails of this garnet grain also indicates independently a significant pure shear (interpretation as per Spry 1969). A lenticular hornblende fish devoid of pressure shadow/rim/mantle (Fig. 13c) exemplifies "naked clast" of Passchier and Trouw (2005) that can develop more efficiently than feldspar grains (Trouw et al. 2010). When such naked clasts are defined by minerals with one set of cleavage planes, such as micas (Fig. 13d), the ductile shear sense has commonly been deduced from inclination of cleavage planes, and not from the near-symmetric shape of the clast. This is also a case of marginal recrystallization at the boundary of the lenticular mica fish, as described by ten Grotenhuis et al. (2003) and Mukherjee (2011a, b). The thin zone of recrystallization presumably escaped ductile shear.

Boudins with symmetric clasts seem to be more common with lenticular boudin geometry (Fig. 14a). This is similar to case 3 of symmetric boudin in Fig. 10 by Lacassin (1988) where foliation in the matrix parallels the long axis of the lenticular boudinaged clast. Asymmetric mineral fish might get boudinaged/fractures into near-symmetric

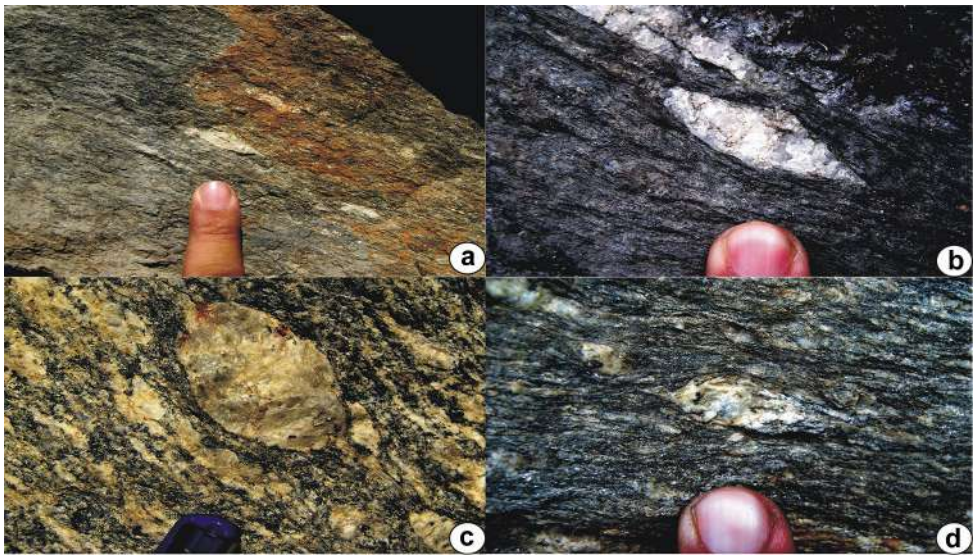

Fig. 12 Augen of different geometries. From gneisses of Greater Himalayan Crystallines, Bhagirathi river section, Uttarakhand, India. Reproduced from Mukherjee (2014). **a** Lenticular. Reproduced from Fig. 3.5 of Mukherjee (2014). **b** Rhombic. Reproduced from Fig. 3.2 of Mukherjee (2014). **c** Lenticular with rather low aspect ratio. Reproduced from Fig. 3.22 of Mukherjee (2014). **d** Lenticular but with a central minor pinch. Reproduced from Fig. 3.13 of Mukherjee (2014)

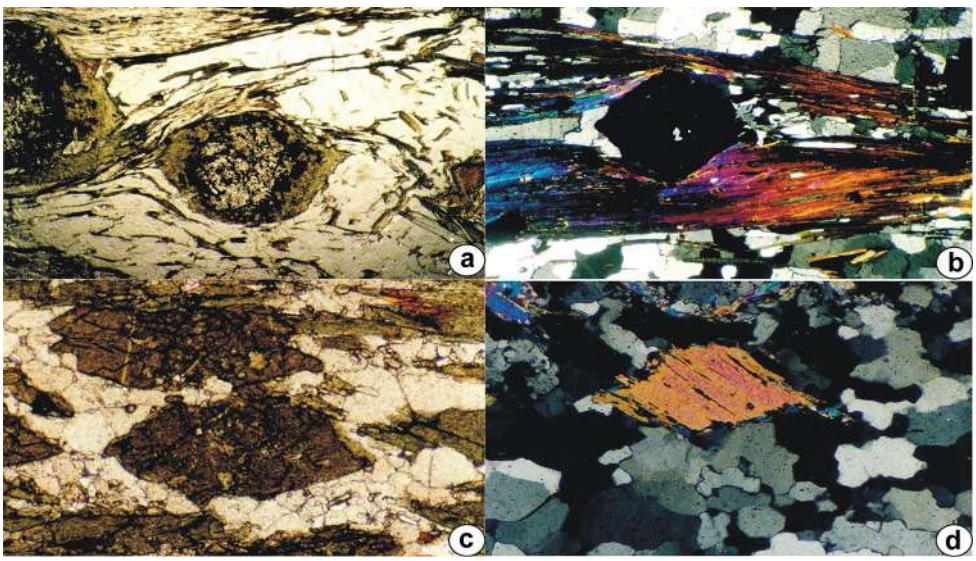

Fig. 13 **a** Chlorite rims near symmetrically a retrogressed garnet. Plane-polarized light. Photograph length: 4 mm. From Tso Morari dome, Ladakh region, India. Reproduced from Fig. 1.58 of Mukherjee (2013a, b, c, d). **b** Squarish garnet grain that looks internally undeformed. Cross-polarized light. Photograph length: 4 mm. Reproduced from Fig. 1.76 of Mukherjee (2013a, b, c, d). **c** A lenticular hornblende fish/augen. Plane-polarized light. Photograph length: 4 mm. From Shyok Suture Zone, Ladakh region, India. Reproduced from Fig. 1.68 of Mukherjee (2013a, b, c, d). **d** Cross-polarized light. Photograph length: 4 mm. Reproduced from Fig. 1.64 of Mukherjee (2013a, b, c, d)

rhombic clasts that individually do not show shear sense (Fig. 14b). To deduce shear sense in this case prior to boudinaging, one needs to reconstruct the broken grains, and visualize the fish geometry in totality. Bulged veins in mesoscale sometimes show minor pinching near the central part (Fig. 14c). Figures 12c and 14c are the cases where Ramberg's (1952) and Cosgrove's (2007) mechanism of pure shear might work to produce those shapes. Pure shear has been deciphered from the Greater Himalayan Crystallines rocks from the Sutlej river section (Grasemann et al. 1999; Law et al. 2010; Mukherjee and Koyi 2010a) from where Figs. 12c and 14c come. Sometimes, the vein near the main bulge also shows minor symmetric swells and pinches (Fig. 14d). This resembles few of the model generated boudins in Fig. 11 by Abe and Urai (2012).

Veins that cut across main foliations could be symmetric and do not reveal shear sense. Figure 15a shows a thick and nearly rectangular vein that cuts across a leftward dipping

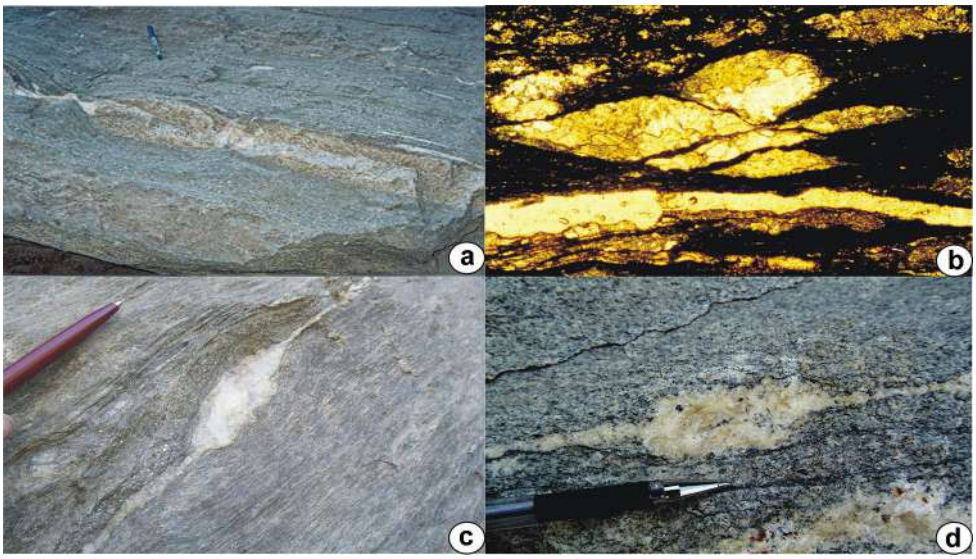

Fig. 14 Broken/boudinaged clasts. **a** Lenticular boudin of granitic melt with prominent scar folds. Secondary quartz filling in inter-boudin space. Near Karcham, Sutlej section of Main Central Thrust Zone, Himachal Pradesh, India. **b** A sigmoid calcite fish fractured into a symmetric rhombic shape. Cross-polarized light. Photograph length: 2 mm. From mylonite of Pangong Tso Group, Ladakh, India. Reproduced from Fig. 12d of Mukherjee (2011a, b). **c** A swelled up vein of quartz inside mylonite with minor pinch nearly at the central part. Near Jhakri, Sutlej section of Greater Himalayan Crystallines, Himachal Pradesh, India. **d** Same as previous situation, but the tail/vein from the main swelled body of quartz also shows minor pinches and swells. At the opposite bank of Sutlej river of Jhakri hydroelectric power station. Sutlej section of Greater Himalayan Crystallines, Himachal Pradesh, India

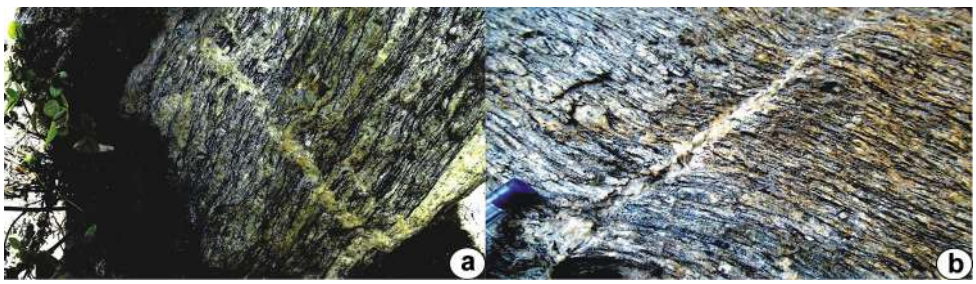

Fig. 15 **a**, **b** Quartz vein across gneissic main foliation. At the opposite bank of Sutlej river of Jhakri hydroelectric power station. Sutlej section of Greater Himalayan Crystallines, Himachal Pradesh, India

main gneissic foliation. Interestingly, (1) The quartz vein continues along the main foliation along its numerous branches; and (2) Near the vein, no significant deflection of the main foliations is noted. In contrary, symmetric veins (Fig. 15b) (1) not always have continuation inside the main foliation; and (2) can show drag effects of main foliation near its length, defining classical flanking structures (Passchier 2001; Mukherjee and Koyi 2009; Mukherjee 2011b, 2014).

Conclusions

Ductile shear zones may consist of symmetric augen, lenticular mineral fish, clasts with or without mantles/wings/tails, lozenges, boudins, veins and folds in a wide range of rock types. Symmetric augen, clasts, lozenges and boudinaged clasts can have a number of shapes such as lenticular, sub-circular, euhedral, rectangular, rhombic, squarish, etc. The now symmetric clasts in ductile shear zones were possibly oriented orthogonal to the stress direction, underwent pure shear, and attained symmetric shapes (as in Treagus and Lan 2000). Augen can have syntectonic or post-tectonic growth, can act as a porphyroblast or even a porphyroclast, may have magmatic origin, and might be defined by more competent minerals. More competent minerals such as hornblende over feldspar develop naked clasts more feasibly. Separate analog and numerical modeling and microstructural observations indicate that the degree of symmetry and geometry of clast and mantle geometries by ductile shear depends on (1) the flow pattern developed within the matrix; (2) matrix rheology: whether Newtonian or non-Newtonian; (3) rheological contrast between the clasts and the matrix; (4) degree of slip of clasts within the matrix; (5) variation of rate of shear across shear zone; (6) deformation temperature; and (7) shear intensity. For

example, winged clasts form when the mantle and the matrix are of nearly the same competency. Coiled mantles develop in more viscous media. However, how all the seven constraints can govern the shape asymmetry of clasts simultaneously is not known. Additionally, the mantle/wing geometry is primarily controlled by (1) the initial aspect ratio of the clast; (2) rate of fall of clast size; (3) ratio of simple-to-pure shear; and (4) relative rates of crystallization and strain. Recrystallization of clasts can supply materials for mantle and help transform a delta structure into a phi-structure, and then into a sigma structure. A slow recrystallization rate, on the other hand, can produce a theta structure. Pure shear can produce symmetric pressure shadows, fringes and augen. Lower curvature of tails can indicate a pure shear. Symmetric lozenges form for certain angular relation between shear zone and planes of anisotropy in rocks, and that between cross-cutting shear zones. Ductile shear sense might still be deduced from symmetric clasts by noting either any quarter fold of matrix foliation formed around clasts, or sigmoidal nature of the inclusion pattern (S-internal) inside them.

Extension of a non-Newtonian matrix with non-Newtonian clasts embedded develops symmetric necking around clasts. Asymmetry develops upon intense extension. Near-symmetric bone-shaped boudins might be produced by rotation of veins. Pure shear can produce highly convex bulging symmetric boudins (Maeder et al. 2009). False/pseudo boudins may be symmetric and lenticular. Orthorhombic symmetric boudins produce by no slip of inter-boudin surfaces. Unlike clasts, matrix rheology may not decide geometry of all kinds of (foliation) boudins. Extensional stress parallel to foliation planes can develop symmetric pinch and swell structures, and compressional stress symmetric folds. Parasitic folds of a lower order fold not affected by ductile shear are symmetric Newtonian viscous layer under pure shear within a non-Newtonian matrix may form symmetric folds. Post-tectonic veins cutting across main foliations (primary shear C planes) and do not give shear sense.

Natural examples of symmetric objects from Himalayan ductile shear zones show internal foliations inside augen concordant with the matrix foliation. Symmetric lenticular objects with high aspect ratios might indicate pronounced ductile shear and might have a previous asymmetric shape. Tails of centrally pinched augen might also show minor pinches. Chemical alterations such as retrogression of minerals can supply mantle materials. Pinches in tails and symmetric pressure shadows in Greater Himalayan Crystallines indicate their pure shear origin, which matches with an already established component of pure shear from this terrain. Asymmetric mineral fish might get fractured to produce near-symmetric pieces. Understanding symmetric structures, in ductile shear zones of different geometries (Mukherjee 2012, Mukherjee et al. 2012; Mukherjee and Biswas 2014, 2015) can better explain tectonics (e.g. Mukherjee et al. 2013, 2015a, b, 2016; Misra and Mukherjee 2016).

Acknowledgments IIT Bombay funded partially. Ripun Kumar Gogoi (IIT Bombay) prepared few diagrams. Reviewer: David Iacopini. Editors: Karel Schulmann, Christian- and Monika Dullo.

References

Abe S, Urai JL (2012) Discrete element modeling of boudinage: insights on rock rheology, matrix flow, and evolution of geometry. J Geophys Res. doi:10.1029/2011JB008555

Arslan A, Passchier CW, Koehn D (2008) Foliation boudinage. J Struct Geol 30:291–309

Augustithis SS (1979) Atlas of the textural patterns of basic and ultrabasic rocks and their genetic significance. Walter de Gruyter, Berlin, pp 17–107

Awdal A, Healy D, Alsop GI (2014) Geometrical analysis of deformation band lozenges and their scaling relationships to fault lenses. J Struct Geol 66:11–23

Barbour GP (1930) Origin of the Bedford augen-gneiss. Am J Sci 219:351–358

Bard JP (1986) Microtextures of igneous and metamorphic rocks. Reidel, Dordrecht, p 87

Barker AJ (1998) Introduction to metamorphic textures and microstructures, 2nd edn. Stanley Thornes (Publishers) Ltd., Cheltenham

Bellot J-P, Bronner G, Laverne C (2002) Transcurrent strain partitioning along a suture zone in the Maures massif (France): result of an eastern indenter tectonics in European Variscides? In: Martínez Catalán JR, Hatcher RD, Arenas R Jr, Díaz Garcıa F (eds) Variscan–Appalachian dynamics: the building of the late Paleozoic basement, vol 364. Geol Soc Am Spec Pap, Boudler, pp 223–237

Bjornerud M (1989) Toward a unified conceptual framework for shear sense indicators. J Struct Geol 11:1045–1049

Bons PD, Barr TD, ten Brink CE (1997) The development of d-clasts in non-linear viscous materials: a numerical approach. Tectonophysics 270:29–41

Bons PD, Druguet E, Hamann I, Carreras J, Passchier CW (2004) Apparent boudinage in dykes. J Struct Geol 26:625–636

Bons PD, Druguet E, Castano L-M, Elburg MA (2008) Finding what is now not there anymore: recognizing missing fluid and magma volumes. Geology 36:851–854

Bose S, Marques FO (2004) Controls on the geometry of tails around rigid circular inclusions: insights from analogue modelling in simple shear. Tectonophysics 26:2145–2156

Bouchez JL, Lister GS, Nicolas A (1987) Fabric asymmetry and shear sense in movement zones. Geol Rund 72:401–419

Bucher K, Grapes R (2011) Petrogenesis of metamorphic rocks. Introduction and general aspects of metamorphism. Part I. Springer, Berlin

Cannon RT (1964) Porphyroblastic and augen gneisses in the bartica assemblage, British Guiana. Geol Mag 501:541–547

Chattopadhyay N, Ray S, Sanyal S, Sengupta P (2015) Mineralogical, textural and chemical reconstitution of granitic rock in ductile shear zone: a study from a part of the South Purulia Shear Zone, West Bengal, India. In: Mukherjee S, Mulchrone KF (eds) Ductile shear zones: from micro- to macro-scales. Wiley, Chichester, pp 141–163

Cliff RA, Meffan-Main S (2003) Evidence from Rb-Sr microsampling geochronology for the timing of Alpine deformation in the Sonnblick Dome, SE Taueren Window Australia. In: Vance D, Muller W, Villa IM (eds) Geochronology: Linking the isotropic record with petrology and textures, vol 220. Geological Society London Special, pp 159–172

Cosgrove JW (2007) The use of shear zones and related structures as kinematic indicators: a review. In: Ries AC, Butler RWH, Graham R (eds) Deformation of the continental crust: the legacy of Mike Coward, vol 272. Geol Soc, London, Spec Publ, pp 59–74

Dabrowski M, Grasemann B (2014) Domino boudinage under layer-parallel simple shear. J Struct Geol 68:58–65

Davis GH, Reynolds SJ, Kluth CF (2012) Structural geology of rocks and regions, vol 500, 3rd edn. Wiley, New York, pp 570–571

De Sitter LU (1956) Structural geology. McGraw-Hill, London, p 86

Dell'Angello LN, Tullis J (1989) Fabric development in experimentally sheared quartzites. Tectonophysics 169:1–21

Duretz T, Schmalholz SM (2015) From symmetric necking to localized asymmetric shearing: the role of mechanical layering. Geology 43:711–715

Fry N (1997) The field description of metamorphic rocks. Geological Society of London Handbook. Wiley, Chichester

Ghosh SK (1993) Structural geology: fundamentals and modern developments. Pergamon Press, Oxford **387**

Goscombe BD, Passchier CW (2003) Asymmetric boudins as shear sense indicators—an assessment from field data. J Struct Geol 25:575–589

Goscombe BD, Passchier CW, Hand M (2004) Boudinage classification: end-member boudin types and modified boudin structures. J Struct Geol 26:739–763

Grasemann B, Dabrowski M (2015) Winged inclusions: pinch-and-swell objects during high-strain simple shear. J Struct Geol 70:78–94

Grasemann B, Fritz H, Vannay J-C (1999) Quantitative kinematic flow analysis from the main central thrust zone (NW-Himalaya, India): implications for a decelerating strain path and the extrusion of orogenic wedges. J Struct Geol 21:837–853

Hanmer S, Passchier CW (1991) Shear sense indicators: a review. Geol Surv Can Pap 90:1–71

Hills ES (1963) Elements of structural geology. Methuen and Co Ltd., London, p 302

Hobbs B, Ord A (2014) Structural geology: the mechanics of deforming metamorphic rocks. Principles, vol 1. Elsevier, Amsterdam, pp 1–665

Hollocher K (2014) A pictorial guide to metamorphic rocks in the field. CRC Press, New York, p 174

Hooper RJ, Hatcher RD Jr (1988) Mylonites from the Towaliga fault zone, central Georgia: products of heterogeneous non-coaxial deformation. Tectonophysics 152:1–17

Ishii K (1995) Estimation of non-coaxiality from crinoid-type pressure fringes: comparison between natural and simulated examples. J Struct Geol 17:1267–1278

Ishii K, Kanagawa K, Shigematsu N et al (2007) High ductility of K-feldspar and development of granitic banded ultramylonite in the Ryoke metamorphic belt, SW Japan. J Struct Geol 29:1083–1098

Jain AK, Singh S (2008) Tectonics of the southern Asian Plate margin along the Karakoram Shear Zone: constraints from field observations and U-Pb SHRIMP ages. Tectonophysics 451:186–205

Kanagawa K (1996) Simulated pressure fringes, vorticity, and progressive deformation. In: de Paor DG (ed) Structural geology and personal computers. Elsevier, Oxford

Kenis I, Urai JL, Sintubin M (2006) The development of bone-shaped structures in initially segmented layers during layer-parallel extension: numerical modelling and parameter sensitivity analysis. J Struct Geol 28:1183–1192

Koehn D, Aerden DGAM, Bons PD et al (2001) Computer experiments to investigate complex fibre patterns in natural antitaxial strain fringes. J Meta Geol 19:217–232

Kornprobst J (2002) Metamorphic rocks and their geodynamic significance—A petrological handbook. Kluwer Academic Publishers, Netherlands

Lacassin R (1988) Large scale foliation boudinage in gneisses. J Struct Geol 10:643–647

Law R, Stahr III DW, Ahmad T et al. (2010) Deformation temperatures and flow vorticities near the base of the greater Himalayan Crystalline Sequence, Sutlej Valley and Shimla Klippe, NW India. In Leech ML et al. (eds) Proceedings for the 25th Himalaya-Karakoram-Tibet Workshop. U.S. Geological Survey, Open-File Report 2010–1099, p 2

Le Hebel F, Gapais D, Fourcade S, Capdevila R (2002) Fluid-assisted large strains in a crustal-scale décollement (Hercynian Belt of South Brittany, France). In: De Meer S, Drury MR, De Bresser JHP, Pennock GM (eds) Deformation mechanisms, rheology and tectonics: current status and future perspectives, vol 200. Geol Soc, London, Spec Publ, pp 85–101

Leiss B, Groger HR, Ullemeyer K, Lebit H (2002) Textures and microstructures of naturally deformed amphibolites from the northern Cascades, NW USA: methodology and regional aspects. In: de Meer S, Drury MR, de Bresser JHP, Pennock GM (eds) Deformation mechanisms, rheology and tectonics: current status and future perspectives, vol 200. Geol Soc, London, Spec Publ, pp 219–238

Lister GS, Snoke AW (1984) S-C Mylonites. J Struct Geol 6:617–638

Maeder X, Passchier CW, Koehn DL (2009) Modelling of segment structures: boudins, bone-boudins, mullions and related single- and multiphase deformation features. J Struct Geol 31:817–830

Malavielle J, Lacassin R (1988) 'Bone-shaped' boudins in progressive shearing. J Struct Geol 10:335–345

Mandal N, Samanta SK, Chakraborty C (2000) Progressive development of mantle structures around elongate porphyroclasts: insights from numerical models. J Struct Geol 22:993–1008

Mandal N, Samanta SK, Chakraborty C (2004) Problem of folding in ductile shear zones: a theoretical and experimental investigation. J Struct Geol 26:475–489

Marques FO, Taborda R, Bose S et al (2005) Effects of confinement on matrix flow around a rigid inclusion in viscous simple shear: insights from analogue and numerical modeling. J Struct Geol 27:379–396

Mason R (1978) Petrology of the metamorphic rocks. George Allen & Unwin, London

Masuda T, Mizuno N (1995) Deflection of pure shear viscous flow around a rigid spherical body. J Struct Geol 17:1615–1629

Menegon L, Pennacchioni G, Stünitz H (2006) Nucleation and growth of myrmekite during ductile shear deformation in metagranites. J Metamorph Geol 24:553–568

Menegon L, Pennacchioni G, Spiess R (2008) Dissolution-precipitation creep of K-feldspar in mid-crustal granite mylonites. J Struct Geol 30:565–579

Misra AA, Mukherjee S (2016) Dyke-brittle shear relationships in the Western Deccan Strike Slip Zone around Mumbai (Maharashtra, India). In: Mukherjee S, Misra AA, Calvès G, Nemčok M (eds) Tectonics of the Deccan large Igneous Province. Geological Society, London, Special Publications

Mukherjee S (2011a) Mineral Fish: their morphological classification, usefulness as shear sense indicators and genesis. Int J Earth Sci 100:1303–1314

Mukherjee S (2011b) Flanking Microstructures from the Zanskar Shear Zone, NW Indian Himalaya. YES Bull 1:21–29

Mukherjee S (2012) Simple shear is not so simple! Kinematics and shear senses in Newtonian viscous simple shear zones. Geol Mag 149:819–826

Mukherjee S (2013a) Deformation microstructures in rocks. Springer, Berlin
Mukherjee S (2013b) Channel flow extrusion model to constrain dynamic viscosity and Prandtl number of the Higher Himalayan Shear Zone. Int J Earth Sci 102:1811–1835
Mukherjee S (2013c) Higher Himalaya in the Bhagirathi section (NW Himalaya, India): its structures, backthrusts and extrusion mechanism by both channel flow and critical taper mechanisms. Int J Sci 102:1851–1870
Mukherjee S (2013d) Symmetric and near-symmetric objects in ductile shear zones- examples from Higher Himalaya, Bhagirathi section, India. Geophys Res Abs 15:2585
Mukherjee S (2014) Atlas of shear zone structures in meso-scale. Springer, Cham
Mukherjee S (2015) Atlas of structural geology. Elsevier, Amsterdam
Mukherjee S, Biswas R (2014) Kinematics of horizontal simple shear zones of concentric arcs (Taylor Couette flow) with incompressible Newtonian rheology. Int J Earth Sci 103:597–602
Mukherjee S, Biswas R (2015) Biviscous horizontal simple shear zones of concentric arcs (Taylor Couette flow) with incompressible Newtonian rheology. In: Mukherjee S, Mulchrone KF (eds) Ductile shear zones: from micro- to macro-scales. Wiley, Chichester, pp 59–62
Mukherjee S, Koyi HA (2009) Flanking microstructures. Geol Mag 146:517–526
Mukherjee S, Koyi HA (2010a) Higher Himalayan Shear Zone, Sutlej section: structural geology and extrusion mechanism by various combinations of simple shear, pure shear and channel flow in shifting modes. Int J Earth Sci 99:1267–1303
Mukherjee S, Koyi HA (2010b) Higher Himalayan Shear Zone, Zanskar Indian Himalaya: microstructural studies and extrusion mechanism by a combination of simple shear and channel flow. Int J Earth Sci 99:1083–1110
Mukherjee S, Mulchrone KF (2012) Estimating the viscosity and Prandtl number of the Tso Morari crystalline gneiss dome, Indian western Himalaya. Int J Earth Sci 101:1929–1947
Mukherjee S, Mulchrone KF (2013) Viscous dissipation pattern in incompressible Newtonian simple shear zones: an analytical model. Int J Earth Sci 102:1165–1170
Mukherjee S, Koyi HA, Talbot CJ (2012) Implications of channel flow analogue models for extrusion of the Higher Himalayan Shear Zone with special reference to the out-of-sequence thrusting. Int J Earth Sci 101:253–272
Mukherjee S, Mukherjee B, Thiede R (2013) Geosciences of the Himalaya-Karakoram-Tibet Orogen. Int J Earth Sci 102:1757–1758
Mukherjee S, Carosi R, van der Beek PA et al (2015a) Tectonics of the Himalaya: an introduction. Geol Soc London Specl Publ 412:1–3
Mukherjee S, Punekar J, Mahadani T, Mukherjee R (2015b) Intrafolial folds: review and examples from the western Indian Higher Himalaya. In: Mukherjee S, Mulchrone KF (eds) Ductile shear zones: from micro- to macro-scales, 1st edn. Wiley, Chichester, pp 182–205
Mukherjee S, Misra AA, Calvès G et al. (2016) Tectonics of the Deccan Large Igneous Province: an introduction. Geological Society London Special Publications, London (in press)
Mulchrone KF, Mukherjee S (2015) Shear Senses and Viscous Dissipation of Layered Ductile Simple Shear Zones. Pure appl Geophys 172:2635–2642
Nabelek PI, Whittington AG, Hofmeister AM (2010) Strain heating as a mechanism for partial melting and ultrahigh temperature metamorphism in convergent orogens: implications of temperature dependent thermal diffusivity and rheology. J Geophys Res 115:B12417
Nicolas A (1987) Principles of rocks deformation. D. Reidel Publishing Company, Dordrecht, p 88
Ord A, Hobbs B (2013) Localized folding in general deformations. Tectonophysics 583:30–45
Passchier CW (1994) Mixing in flow perturbations: a model for development of mantled porphyroclasts in mylonites. J Struct Geol 16:733–736
Passchier CW (2001) Flanking structures. J Struct Geol 23:951–962
Passchier CW (2008) Pseudo-boudins in Pegmatite, Arunta, Australia. J Struct Geol 30:273
Passchier C, Coelho S (2006) An outline of shear-sense analysis in high-grade rocks. Gond Res 10:66–76
Passchier CW, Sokoutis D (1993) Experimental modelling of mantled porphyroclasts. J Struct Geol 15:895–909
Passchier CW, Trouw RAJ (2005) Microtectonics, 2nd edn. Springer, Berlin
Passchier CW, Myers JS, Kroner A (1990) Field Geology of High-Grade Gneiss Terrains. Springer, Berlin
Philips E (2006) Micromorphology of a debris flow deposit: evidence of basal shearing, hydrofracturing, liquefaction and rotational deformation during emplacement. Quater Sci Rev 25:720–738
Ponce C (2014) Structural analyses of tectonic lozenges in anisotropic rocks: field analysis and experimental modelling. Ph.D. Thesis. Universitat Autonoma de Bercelona. pp. 1–141
Ponce C, Druguet E, Carreras J (2013) Development of shear zone-related lozenges in foliated rocks. J Struct Geol 50:176–186
Ramberg H (1952) The origin of metamorphic and metasomatic rocks. The University of Chicago Press, Chicago, pp 233–234
Ree J-H, Kim HS, Han R, Jung H (2005) Grain-size reduction of feldspars by fracturing and neocrystallization in a low-grade granitic mylonite and its rheological effect. Tectonophysics 407:227–237
Regenauer-Lieb K, Yuen DA (2003) Modeling shear zones in geological and planetary sciences: solid- and fluid-thermal–mechanical approaches. Earth Sci Rev 63:295–349
Roshoff K (1979) Deformation structures in the Tannas augen gneiss. In: Easterling KE (ed) Mechanism of deformation and fracture. Pergamon Press Ltd., Oxford, pp 159–172
Simpson C, Schmid SM (1983) An evaluation of criteria to deduce the sense of movement in sheared rocks. Geol Soc Am Bull 94:1281–1288
Simpson C, Winsch RP (1989) Evidence for deformation-induced K-feldspar replacement by myrmekite. J Metamorph Geol 7:261–275
Smith JV (1974) Feldspar minerals: chemical and textural properties. Springer, Berlin
Spry A (1969) Metamorphic textures. Pergamon Press, Oxford, pp 242–247
Spry A (1974) Metamorphic textures. Pergamon Press, Oxford, pp 240–246
ten Grotenhuis SM, Trouw RAJ, Passchier CW (2003) Evolution of mica fish in mylonitic rocks. Tectonophysics 372:1–21
Treagus S, Lan L (2000) Pure shear deformation of square objects, and applications to geological strain analysis. J Struct Geol 22:105–122
Treagus S, Lan L (2003) Simple shear of deformable square objects. J Struct Geol 25:1993–2003
Trouw RAJ, Passchier CW, Wiersma DJ (2010) Atlas of Mylonites-and related microstructures. Springer, Berlin
Turner FJ, Verhoogen J (1951) Igneous and metamorphic petrology. McGraw Hill, New York, p 61
van der Wateren FM, Kluiving SJ, Bartek LR (2000) Kinematic indicators of subglacial shearing. In: Maltman AJ, Hubbard B, Hambrey MJ (eds) Deformation of glacial materials, vol 176. Geol Soc, London, Spec Publ, pp 259–278

Vernon RH (1986) K-feldspar megacrysts in granites- phenocrysts not porphyroblasts. Earth Sci Rev 23:1–63

Vernon R (1990) K-feldspar augen in felsic gneisses and mylonites—deformed phenocrysts or porphyroblasts? Geologiska Foreningens i Stockholm Forhandlingar 112:157–167

Vernon RH (2004) A practical guide to rock microstructure. Press Syndicate of the University of Cambridge, Cambridge

Vernon RH, Clarke GL (2008) Principles of metamorphic petrology. Cambridge University Press, New York, pp 326–345

Vidal JL, Kubin L, Debat P, Soula JC (1980) Deformation and dynamic recrystallization of K-feldspar augen in orthogneiss from Montagne Noire, Occitania, Southern France. Lithos 13:247–255

White SH (2010) Mylonites: lessons from Eriboll. In: Law RD, Butler RWH, Holdsworth RE, Krabbendam M, Strachan RA (eds) Continental tectonics and mountain building: the legacy of peach and horne, vol 335. Geol Soc, London, Spec Publ, pp 505–542

Whitten EHT (1966) Structural geology of folded rocks. Rand McNally & Company, Chicago, p 306

Winter JD (2009) Principles of igneous and metamorphic petrology, 2nd edn. Prentice Hall, New Jersey, p 473

Yin A (2006) Cenozoic tectonic evolution of the Himalayan orogen as constrained by along-strike variation of structural geometry, extrusion history, and foreland sedimentation. Earth Sci Rev 76:1–131